



OPEN Effect of steel fiber content on fatigue performance of high-strength concrete beams

Ming Zhang¹✉, Jiahua Jing² & Shike Zhang^{1,2}

This study focuses on the fatigue performance of steel fiber reinforced high-strength concrete structures. The effect of steel fiber volume fraction (0%, 0.5%, 1.0%, 1.5%) on the cracking resistance, deformation characteristics and fatigue life of high-strength concrete beams under fatigue loading were systematically investigated through equal-amplitude fatigue tests on four beam specimens. The results show that the incorporation of steel fibers can significantly improve the crack resistance of concrete, which is manifested in the reduction of crack width by 35–121%. Meanwhile, the steel fibers can effectively inhibit the development of deflection of beams during fatigue loading, slow down the rate of stiffness degradation. The incorporation of steel fibers reduced the mid-span deflection of the beams by 15–61% and increased the fatigue life by 66.9–149.9%. Based on the experimental data, this study confirms that the steel fiber reinforcement technology is a practical and economically significant fatigue performance enhancement solution for high-strength concrete structures. This paper provides an important theoretical basis and technical support for the engineering application of steel fiber reinforced high-strength concrete structures in complex loading environments.

Keywords Fatigue, Steel fiber, High-strength concrete beams, Crack resistance, Deflection, Fatigue life

The expanding application of high-strength concrete in cyclically loaded infrastructures – including offshore platforms, nuclear containment structures, heavy-haul railway systems, and aerospace launch facilities – has positioned fatigue-induced failure as a pivotal concern in modern engineering design. Unlike static failure modes, materials subjected to cycle magnitude alternating stresses exhibit progressive crack propagation that frequently culminates in catastrophic brittle fracture without precursor warnings, representing a critical degradation mechanism threatening structural integrity throughout service life. Notably, steel fiber reinforcement induces remarkable strain-hardening behavior in concrete matrices, achieving 50–150% enhancement in tensile capacity and reduction in crack width, thereby establishing steel fiber reinforced high-strength concrete as an exemplar of next-generation ductile construction materials. Amidst the global acceleration of transportation infrastructure development, major engineering projects worldwide are confronting unprecedented fatigue challenges: China's "Eight Vertical and Eight Horizontal" high-speed rail network operates at a density exceeding 480 trains/day, the EU's Trans-European Transport Network (TEN-T) mandates core rail speeds ≥ 250 km/h, North American heavy-haul railways now handle 36-ton axle loads, and Southeast Asian transnational railways endure 45 °C cyclic hygrothermal stresses. These extreme service conditions have reduced the fatigue life of conventional concrete beams to less than 40% of design requirements, with 27 documented fatigue-induced speed restriction incidents in global rail systems between 2020 and 2024. The need to expand the use of steel-fiber concrete and steel-fiber high-strength concrete in these transport projects makes the study of their fatigue properties an issue that cannot be ignored.

Fatigue mechanics, since its conceptualization by German engineer W.A.J. Albert in 1829, has evolved into a critical discipline across transportation and structural engineering domains. While early concrete infrastructure rarely encountered fatigue failures due to conservative allowable stress designs, the advent of high-strength concrete and intensive cyclic loading in modern transportation systems (e.g., 30,000+ daily truck passages on bridges over motorways) has exposed critical durability gaps^{1,2}. Particularly concerning is the brittle fracture pattern observed in building structures under fatigue loading, where failure occurs abruptly at merely 50–60% of ultimate static capacity. The emergence of steel fiber concrete has opened up a revolutionary path to overcome the century-old problem of fatigue damage in engineering structures—through the cross-scale enhancement of discrete fibers, a three-dimensional stress transfer network is constructed within the concrete matrix, and

¹School of Civil Engineering and Architecture, Anyang Normal University, Anyang 455000, China. ²Henan Province Engineering Technology Research Center of Digital Intelligent Building and Low Carbon Building Materials, Anyang Normal University, Anyang 455000, China. ✉email: zm@aynu.edu.cn

its unique crack bridging mechanism can effectively inhibit micro-cracks from sprouting and slow down the expansion of macro-cracks, which will result in a quantum leap in structural fatigue life. Studies^{3–11} have shown that adding steel fibers to concrete can make up for the lack of high-strength concrete performance and improve its ductility and tensile and crack resistance. Because of the excellent performance of steel fiber high-strength concrete, steel fiber high-strength concrete is increasingly being paid great attention to and widely used in road and bridge engineering, construction engineering, water conservancy engineering, and other engineering structures, and vigorously promote the development of concrete materials in the direction of high-strength and high-performance. Scholars around the world are beginning to conduct preliminary research and studies on the fatigue properties of fiber concrete and its structure. The relevant research findings are summarized and collated below:

Research on Material-Level: The fatigue performance of steel fiber reinforced concrete was first systematically studied by Sun Wei and his team¹², who identified that steel fibers inhibit crack propagation under cyclic loading, thereby enhancing fatigue resistance. Fatigue Behavior and Mechanisms: Nanni¹³ examined the flexural fatigue characteristics of steel fiber reinforced concrete, emphasizing residual strength and the role of fiber types. Singh S P^{14–16} conducted comprehensive studies on steel fiber reinforced concrete fatigue resistance using cyclic axial compression and four-point bending tests, providing foundational insights into material behavior. Deng Zongcai^{17,18} investigated the damage mechanisms of plain concrete and steel fiber reinforced concrete under axial compressive fatigue loading. His work also explored the flexural fatigue performance of cellulose fiber, steel fiber, and hybrid fiber concrete, demonstrating a 6.8% increase in fatigue strength for cellulose fiber concrete compared to plain concrete. Additional studies^{19–21} have analyzed steel fiber reinforced concrete fatigue properties from various angles, contributing to a deeper understanding of material performance under cyclic loading. While extensive research has been conducted on steel fiber reinforced concrete materials, studies on structural members, particularly beams, remain scarce, with most focusing on normal-strength concrete.

Research on steel fiber reinforced concrete structural members: Chang D and Chai W²² performed fracture and fatigue tests on 33 steel fiber reinforced concrete beams, evaluating the effects of steel fiber content, aspect ratio, and other parameters on fatigue performance. They also proposed a method for calculating beam fatigue strength. The Zhengzhou University research team^{23,24} has advanced the understanding of fiber-reinforced concrete beams, developing methodologies for calculating crack width, stiffness, and other performance metrics. Recent studies^{25,26} have highlighted the significant influence of steel fiber content on the fatigue performance of concrete, particularly in high-strength applications, underscoring the need for further investigation.

The current research mainly focuses on the compressive fatigue, tensile fatigue and bending fatigue of steel fiber concrete, and the research on the fatigue performance of steel fiber reinforced high-strength concrete and its components is still relatively small. This paper combines the steel fiber high-strength concrete beams through the equal amplitude fatigue test of steel reinforcement, discusses the effect of steel fiber content on the fatigue performance of high-strength concrete beams, systematic analysis of the fatigue damage pattern of high-strength concrete beams in the case of different steel fiber volume fractions, cracks, deflection and stiffness degradation, fatigue life and other changes in the law of change. The study provides important data to support the application of steel fiber reinforced high-strength concrete in structures subjected to fatigue loading effects.

Experiments

Experimental design

Parametric design

A total of one ordinary high-strength concrete beam and three high-strength concrete beams with varying fiber volume fractions (corresponding to fiber volume fractions of 0.5, 1, and 2%, respectively) were designed based on the high-strength concrete with a designed strength of 60 MPa.

Corresponding static loading and isotropic fatigue tests were conducted to determine fatigue performance indexes such as cracking loads, fatigue crack development, fatigue damage patterns, and fatigue life of steel fiber-reinforced high-strength concrete beams. High strength concrete beams reinforced with steel fibers were evaluated for performance indicators, including cracking load, fatigue crack formation, concrete and reinforcement strain variations, fatigue damage pattern, and fatigue life. The design parameters and reinforcement diagrams of the test beams are shown in Table 1; Fig. 1. The length of the test beam was 3 m, The design size of the cross-section of the test beams is 150 mm×300 mm, and the cross-sectional dimensions in the table are measured data before the tests.

Material and concrete mix proportion

Cement P.O.42.5 cement produced by Henan Xinxing Cement Factory is used, which has been tested to meet the technical requirements stipulated.

Beams number	Dimensions of section b (width) ×h (height)	Steel fiber volume fractions V_f	Lower fatigue load limit	Fatigue Load Upper Limit
B0	151 mm×302 mm	0	0.15 M_u	0.5 M_u
BSF05	149 mm×304 mm	0.5%	0.15 M_u	0.5 M_u
BSF10	151 mm×301 mm	1.0%	0.15 M_u	0.5 M_u
BSF15	150 mm×301 mm	1.5%	0.15 M_u	0.5 M_u

Table 1. Specimens parameters. M_u is the ultimate bending moment of the beam.

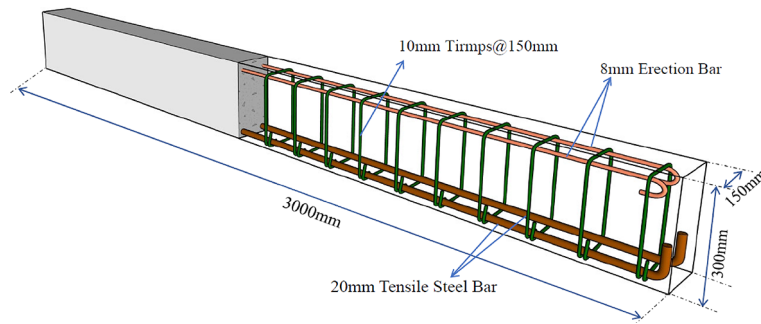


Fig. 1. Dimensions and reinforcement of the beam.



Fig. 2. Steel fiber pictures.

Aggregate The test coarse aggregate is crushed stone from Nanyang, Henan Province, with good grading, particle size ≤ 20 mm, mud content $< 1\%$, which meets the requirements, but due to the configuration of high-strength concrete, the crushed stone should be cleaned and air-dried before use to ensure the pouring quality. The fine aggregate is medium grade river sand with good grading, and the water content is tested according to the specification before the test in order to adjust the proportion accurately.

Water reducing agent Adopt FDN-1 type powder high efficient water reducing agent produced by Henan Building Materials Design and Research Institute, the water reducing efficiency is 18~25%.

Steel fiber The steel fibers were made of cold-drawn end-hooked Jamix steel fibers with an equivalent diameter of 0.55 mm and a length of 35 mm, as shown in Fig. 2.

The mechanical properties and ease of steel fiber concrete and steel fiber high-strength concrete are related to cement strength grade, water-cement ratio, steel fiber volume rate and length-to-diameter ratio, sand rate, water consumption and other factors. Among them, the water-cement ratio and cement strength grade have a greater effect on its compressive strength; the volume rate of steel fibers, length-diameter ratio and cement strength grade have a greater effect on its splitting strength and flexural strength; and the sand rate and water consumption have

Beams number	Cement	Water	Sand	Coarse aggregate	Water reducer	Steel fiber
B0	487	146	618	1199	7.3	0
BSF05	520	156	710	1065	7.8	39
BSF10	547	164	696	1044	8.2	78
BSF15	573	172	682	1023	8.6	117

Table 2. Mix proportion of concrete $/(kg \cdot m^{-3})$.



Fig. 3. Fabrication of beams.

a greater effect on its ease of use. The steel fiber concrete mixing ratio used in this test is determined based on the combination of previous mixing ratio studies, considering the differences in the varieties of raw materials, the moisture content of the materials and site construction conditions, etc., and the components were test-mixed before casting, to determine the basic mechanical properties and working performance, the specific mixing proportion is shown in Table 2.

Preparation of test beams

The production of beams is mainly divided into tying reinforcement, making formwork, mixing, pouring concrete, and curing and demolding (Fig. 3). Use forced mixer mixing during the concrete mixing process to ensure uniform steel fiber distribution and prevent agglomeration. The mixing sequence is as follows: To prevent steel fiber agglomeration, add cement and powdered high-efficiency water reducing agent mixing first, followed by sand and coarse aggregate in turn. The steel fiber will then be gradually dispersed to join the mixing process, and steel rods will be artificially used to aid in the mixing (dry mixing). Water is then added for mixing. Fiber concrete requires a suitable extension of vibration duration; however, excessive vibration should not impact the dispersion of steel fibers. After a day of pouring, the specimens can be demolded, and the members need to be irrigated.

Fatigue test loading procedure and device

Loading procedure

The loading process for the equal-amplitude fatigue test has three stages: the static load test, the fatigue test, and the destructive test, as per the test specification (Standard for Test Methods of Concrete Structures GB50152-2012)²⁷.

- (1) Static load test stage: The static load test stage is performed in accordance with the loading procedure of the static monotonic loading test. Before loading to the fatigue load limit value in a graded manner, the preload is performed, and after determining whether the equipment is normal or not, the static load test is conducted for two loading and unloading cycles. The load of each stage is assumed to be 20% of the fatigue load limit value. Load to the upper limit value of fatigue load, each time to record the steel and concrete strains, as well as the deflection of the beam, and at the same time the test process to record the cracking load and the development of cracks.
- (2) Fatigue test stage: equal-amplitude fatigue test are loaded according to the sinusoidal wave, the loading frequency of 5 Hz, adjust the loading frequency, fatigue load is applied, and repeatedly adjusted to maintain the stability of the load, so that the error is not greater than $\pm 3\%$, the test process, fatigue loading During the test, the fatigue load is cycled to 10,000, 50,000, 100,000, 150,000, 200,000, 500,000, 1,000,000, 1,500,000, 2,000,000 times and then stopped, and then a static load test is carried out in which the upper limit of the fatigue load is loaded and the lower limit of the fatigue load is unloaded. Measure the strain, crack, deflection and its development under each level of loading.
- (3) Destruction test stage: when the test repeated load reaches the required number of loadings 2 million times, if the test beam is still not destroyed, continue to carry out a test specimen static load test until the test beam is destroyed, and record the reinforcement and concrete strain under each level of loading, as well as deflection and deformation of the beam, and measure the residual load carrying capacity of the test beam.

Loading equipment and devices

The structural test hall is used for the test. The test beams must be geometrically aligned and maintain the two supports at the same height. The loading point and the support are all cushioned with steel plate to prevent the occurrence of localized concrete compression damage. The two ends of the test beam use flat rubber bearings to imitate the member's real operating state. The static load test involves synchronous and graduated loads. Jinan Materials Testing Equipment Factory's hydraulic pulsation fatigue testing equipment (PE-50 A) has a maximum dynamic and static load of 50 tons and a frequency range of 100–500 times per minute. Figure 4 shows the loading schematic and equipment.

Basic material property data of concrete and steel reinforcement

Reinforced steel fiber high-strength concrete beam fatigue test before the basic mechanical properties of steel reinforcement and steel fiber concrete test, the main measurement of mechanical property indexes is concrete cubic compressive strength, split tensile strength, axial compressive strength, modulus of elasticity, the yield strength of steel reinforcement, tensile strength, elongation, cold bending properties, and other mechanical indicators. The specimens of the basic mechanical properties of concrete test were cast at the same time with the test beam and maintained under the same conditions as the test beam. The mechanical properties of steel reinforcement and concrete are shown in Tables 3 and 4.

Fatigue performance

Fatigue life

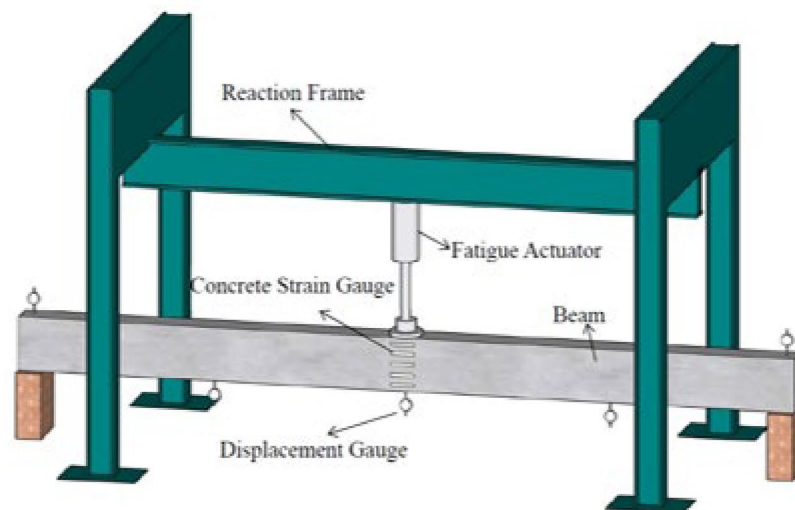
When fatigue damage occurs in the beams, the main cause is the fatigue damage of the reinforcement leading to the failure of the beams. Figure 5 illustrates the typical characteristics of fatigue fracture of reinforcement in beam BSF05. There is no visible necking occurrence in the fatigue damage portion of the reinforcement, which is a typical brittle damage feature. The fatigue life of the test beams in the damage and damage phenomenon is shown in Table 5. In the same fatigue equivalent stress ratio, the same concrete design strength and reinforcement, the fatigue life of concrete beams with 0.5, 1.0 and 1.5% steel fiber volume fractions increased by 66.9, 132.9 and 149.9% respectively compared with that of the beams without steel fiber, which indicates that the addition of steel fibers to reinforced high-strength concrete beams can effectively increase the fatigue life of the beams, and the method of improving the fatigue performance of beams through the incorporation of steel fibers is effective and feasible. As the fatigue cycle progresses, fractures form at the weak places in the concrete material to release energy (the material must remain in a low-energy state). Concurrently, the ability to spread existing fissures deteriorates. Under fatigue stress, the fatigue crack opens and closes in cycles, causing friction and impact between the steel fibers and the matrix interface. From the time the fatigue fracture begins until the specimen breaks, it finds a certain equilibrium, which is moderated by the steel fibers. As fatigue progresses, the matrix interface changes from rough to smooth owing to friction, and this equilibrium is broken when the fibers are removed. This causes the fracture to expand, new fibers to engage throughout the cross-section, and a new equilibrium to be established, which is then shattered again. Throughout the process, the contact between steel fibers and concrete absorbs a large quantity of energy. The existence of steel fiber and their bonding action with concrete are critical to the consumption of fatigue energy.

Fatigue crack development pattern

Figures 6, 7, 8, 9 systematically shown the fatigue damage progression and crack evolution patterns in the test beams. Comparative analysis reveals three characteristics: (1) Initial crack formation ($\leq 10^4$ cycles): vertical cracks appeared rapidly in all specimens, but with restricted crack geometry; (2) Stable crack development (10^4 -



(A) Loading device



(B) Loading schematic diagram

Fig. 4. Loading device and loading schematic diagram.

Reinforcement grade	Caliber	Yield strength /MPa	Tensile strength /MPa	Elongation δ_s	Cold bending performance
HRB400	20	460.2	685.3	24%	Qualified
HPB300	10	335.0	459.9	37%	Qualified
HPB300	8	338.0	450.1	34%	Qualified

Table 3. Results of mechanical properties of reinforcement.

10^5 cycles): crack topography reached 95% maturity at 10^5 cycles. Cracks reach 95% maturity at 10^5 cycles, and no new cracks are observed, although cyclic loading continues; (3) Crack expansion phase ($> 2 \times 10^5$ cycles): crack widths gradually expand at a decreasing rate. The control beams (B0, 0% steel fibers) were less resistant to cracking, with widened average crack spacing and increased extension heights compared to their fiber-reinforced

Beams number	Cubic compressive strength $f_{cu} / N/mm^2$	Splitting strength $f_{t,s} / N/mm^2$	Axial compressive strength $f_{ck0} / N/mm^2$	Modulus of elasticity $E / N/mm^2$
B0	69.48	7.40	60.10	3.87×10^4
BSF05	79.70	6.17	54.90	4.22×10^4
BSF10	69.48	7.40	60.10	4.26×10^4
BSF15	82.28	7.61	62.17	4.33×10^4

Table 4. Results of mechanical properties of high-strength concrete.

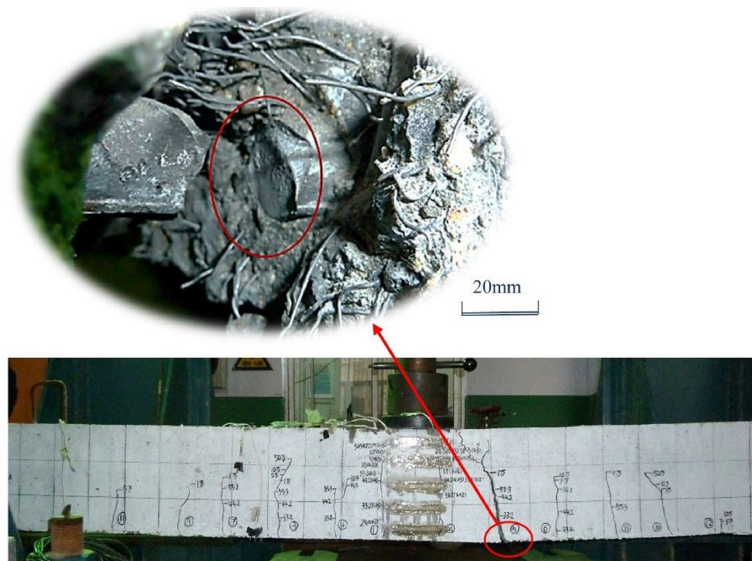


Fig. 5. Typical fatigue damage fracture of reinforcing steel (Beam BSF05).

Beams number	Fatigue life	Destruction phenomenon
B0	54.1×10^4	Fatigue fracture of reinforcement on the north side
BSF05	90.3×10^4	Fatigue fracture of reinforcement on the south side
BSF10	126.2×10^4	Fatigue fracture of reinforcement on the south side
BSF15	135.2×10^4	Fatigue fracture of reinforcement on the south side

Table 5. Fatigue test results.

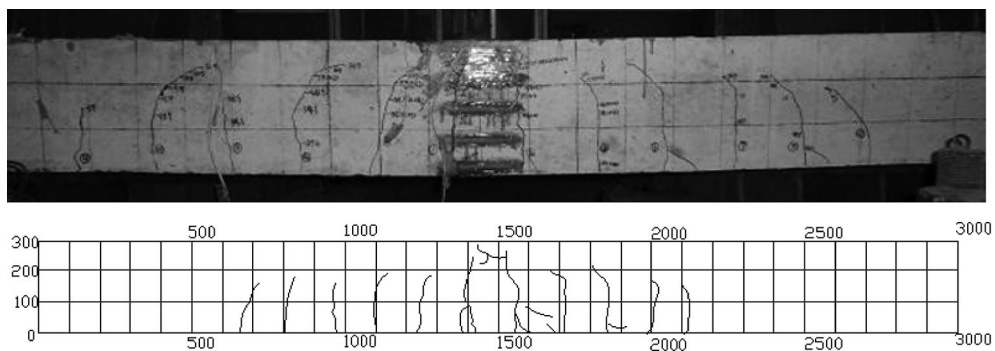


Fig. 6. Diagram of beam B0 damage and cracking.

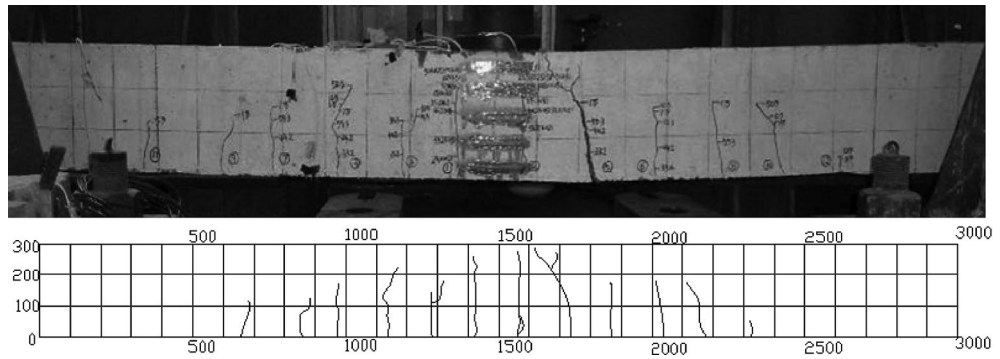


Fig. 7. Diagram of beam BSF05 damage and cracking.

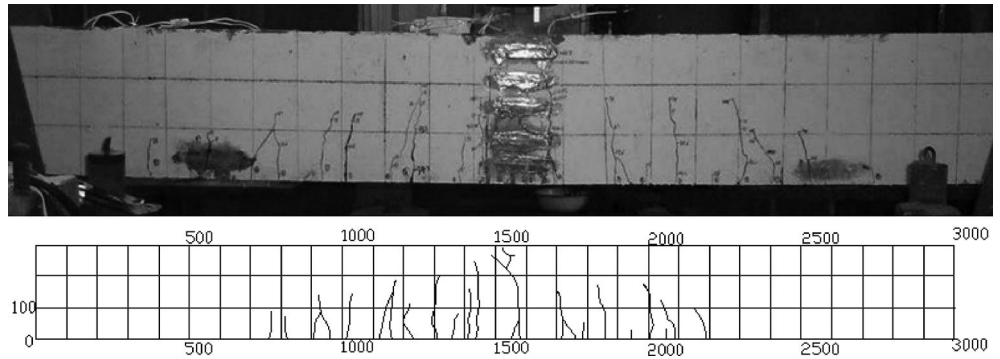


Fig. 8. Diagram of beam BSF10 damage and cracking.

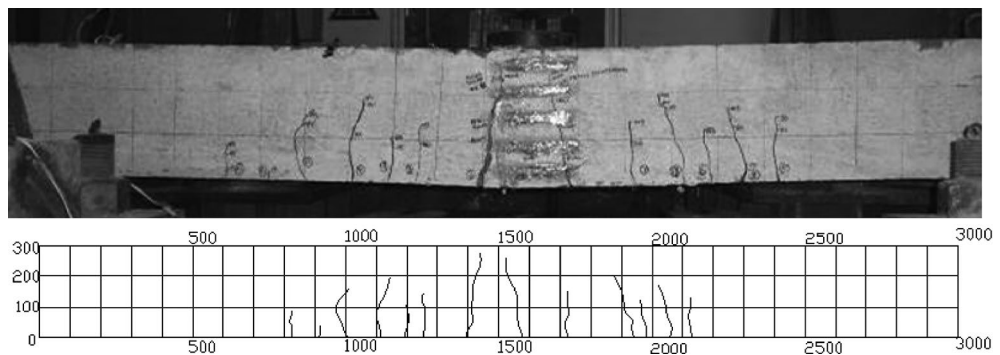


Fig. 9. Diagram of beam BSF15 damage and cracking.

counterparts. The beams containing steel fibers exhibited a refined crack network characterized by high crack density and small crack widths. And with the increase of fiber volume fractions, this trend is more obvious.

Figure 10 depicts the maximum crack width of beams loaded to the fatigue upper limit load after a certain number of fatigue cycles during the test, plotted against the number of cycles. As shown in Fig. 4, fatigue loading, different steel fiber volume fractions series of specimens in the initial 200,000 times of loading, the crack width increased by about 90–120%, with the increase of the volume fractions of steel fibers, the crack width increased with the increase in the number of fatigue cycles, and the magnitude of the increase decreased. When the volume rate of steel fiber reaches 1.5%, steel fiber agglomeration phenomenon occurs in high strength concrete and leads to a decrease in its crack-blocking effect. After the test on the beam span in the destruction of the cross-section to cut, in the destruction of the cross-section of the measured distribution of fibers in the vicinity of the cross-section also confirms the emergence of the phenomenon of agglomeration (shown in Fig. 11). As a result, the amount of steel fibers added to the high-strength concrete mix should be kept to a suitable dosage.

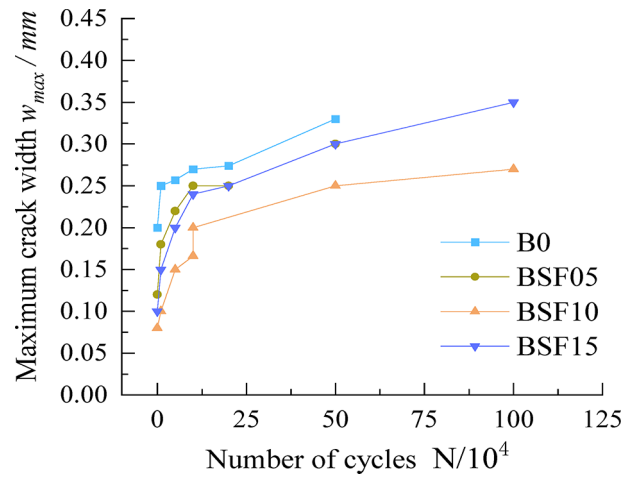


Fig. 10. Maximum crack width development pattern.

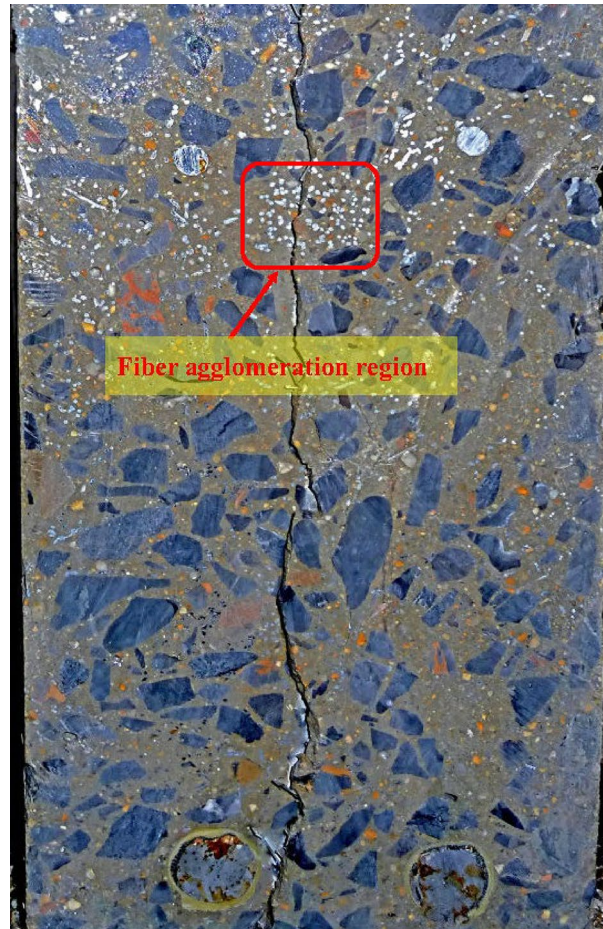


Fig. 11. Phenomenon of agglomeration.

Cumulative residual strain in the compression zone of beams

Concrete under repetitive loading continuously absorbs energy and produces many microcracks in its interior, causing the internal damage of concrete to increase continuously, and these changes in the interior of concrete manifest as increasing residual deformation^{28,29}. The cumulative residual strain reflects the irrecoverable degree of concrete microplastic deformation and microcracks, which is more reflective of the material itself than the maximum deformation. At the same time, different tests have shown that the residual strain of concrete has

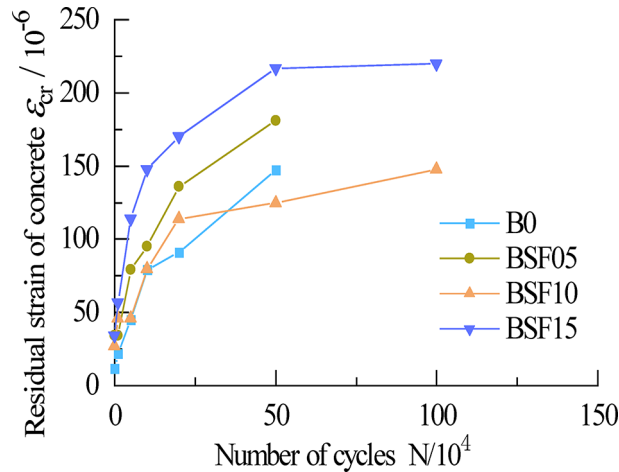


Fig. 12. Development law of the residual strain.

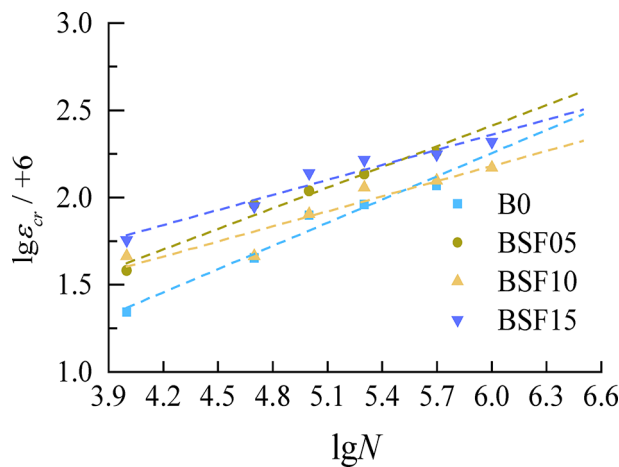


Fig. 13. Double logarithmic curve of cumulative residual strain and fatigue cycles.

good stability and regularity and can better reflect the nonlinear characteristics of concrete fatigue damage, so it is more reasonable to take the cumulative residual strain value of concrete as a macro-physical indicator of concrete fatigue damage to describe the damage state. Previous research on cumulative residual deformation of concrete has mostly concentrated on the axial compression fatigue test of concrete prisms or cylinders, and there is a significant difference between the axial compression of concrete prisms and the concrete stress in the compression zone of the beam. This work systematically measured the residual strain of concrete in the compression zone and analyzed the fatigue load (shown in Fig. 12).

As can be seen from the Fig. 12, the cumulative residual strain of the concrete at the edge of the compression zone of the steel fiber reinforced high-strength concrete beam increases with the increase of the maximum stress level and the number of fatigue cycles, and its development law has an obvious stage. In the early stage of fatigue loading, the cumulative residual strain of concrete in the compression zone develops faster, but its growth rate gradually decreases; after the fatigue cycle reaches a certain number of times, the growth rate of the cumulative residual strain of concrete in the compression zone is basically stable and changes in a linear law. According to previous studies, the development is divided into three stages, and the cumulative residual strain of concrete in the compression zone will enter the rapid development stage again when it is close to destruction. Due to the limitation of test conditions, the development law when approaching damage is not obtained in this paper. It can also be seen from the figure, in the initial 200,000 cycles of loading, different series of steel fiber volume rate of the test beam, with the increase of the volume rate of steel fibers, the cumulative residual strain of the concrete in the compression zone with the increase in the number of fatigue cycles, the cumulative residual strain of the concrete in the compression zone with the increase in the number of fatigue cycles, and its rate of development will be reduced with the incorporation of steel fibers. Figure 13 Double logarithmic treatment of the cumulative residual strain according to the development pattern of the cumulative residual strain shows that the curves exhibit a good linear correlation.

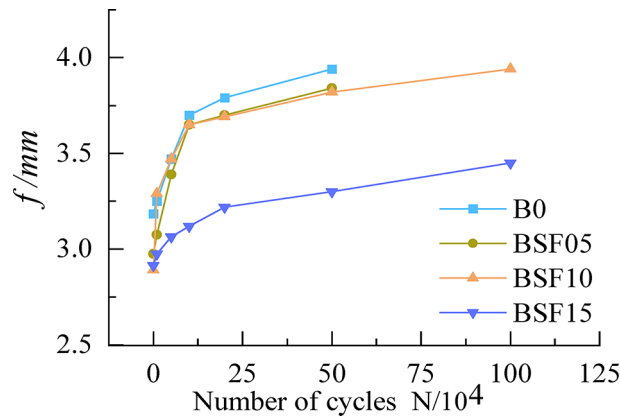


Fig. 14. Changing law of beam mid-span deflection with increasing number of cycles.

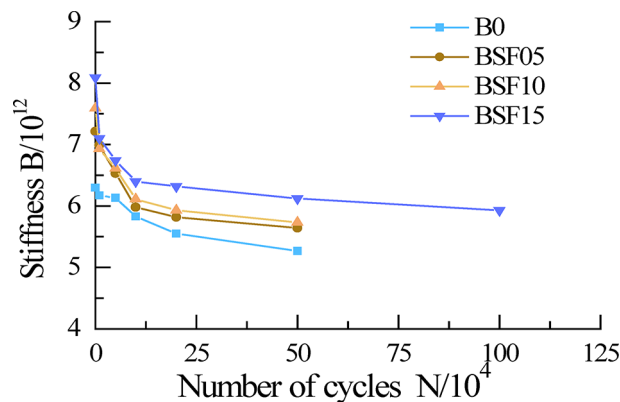


Fig. 15. Stiffness degradation law.

Fatigue deformation properties

Previous research^{4,5,22} has shown that adding fibers to concrete can significantly improve its flexural, cracking, and fatigue resistance. Since there are many factors influencing the fatigue performance of fiber concrete members, including fatigue load characteristics, time course processability, material fatigue characteristics, internal defects, bond characteristics between materials and construction quality, etc., but previous studies mainly focused on unreinforced members, which cannot reflect the development of member deformation and stiffness degradation of actual reinforced members under fatigue load. Figure 14 depicts the variation rule of deflection in the span of reinforced steel fiber high-strength concrete beams under fatigue upper limit load as the number of test cycles increases. The mid-span deflection of steel fiber reinforced high-strength concrete beams grows with the number of cycles. The initial 10,000 times of fatigue load action resulted in a rather quick rise in deflection. However, between 50,000 and 200,000 times, the increase in deflection steadily slowed down. After 200,000 times, the deflection changes stabilized. The figure shows that the deflection of reinforced steel-fiber high-strength concrete beams decreases by 15.0–61.0% when compared to the beams without steel fiber, and the limiting effect of steel fibers on fatigue deformation is especially noticeable for reinforced steel-fiber high-strength concrete beams with higher steel fiber volume fractions. The stiffness loss of reinforced concrete beams under fatigue stress may be classified into three rather visible stages: The residual stiffness decays faster and is unstable at the start of the load cycle, accounting for about 5–10% of the fatigue life; after cycling for a period, the rate of stiffness decay is basically a certain value, accounting for about 80–90% of the fatigue life; and as the fatigue life approaches, the residual stiffness rapidly decreases. As fatigue life approaches, residual stiffness and beam stiffness decline significantly, accounting for approximately 3–5% of total fatigue life.

In this paper, the deflection under different fatigue cycle times is measured during the test, and the flexural stiffness of the section at the corresponding moment is calculated, with a focus on the stiffness change rule of the beam in the first and second stages. According to the test findings, the beam stiffness degradation law is illustrated in Fig. 15. The stiffness decay rate decreases as the volume rate of steel fibers increases. When compared to high-strength concrete beams without the addition of steel fibers, the volume rate of steel fibers of 0.5, 1.0, and 1.5% of the beams stiffness decay rate decreased by 42, 53, and 60%, respectively. The incorporation of steel fibers into high-strength concrete beams can effectively control the stiffness decay rate, limit the cumulative damage of the beams under fatigue loading, and improve the life of the beams.

Beams number	Stiffness decay rate / 10 ⁵
B0	10
BSF05	5.88
BSF10	4.77
BSF15	4.01

Table 6. Stiffness decay rate of the second stage of the beams.

Consistent with the findings of earlier research, the test demonstrates that the residual stiffness degradation rate is fast and unstable at the start of the loading cycle; as the number of cycles increases, the stiffness decay rate decreases and exhibits good linear correlation, and the stiffness degradation enters a relatively stable stage. The stiffness decay rate of the beam in the second stage can be determined based on the test results of the stiffness of the test beam under various fatigue cycle periods since the stiffness decay law of the second stage has a good linear correlation. The stiffness decay rate is the stiffness decay under the unit number of cycles, i.e.

$$k_f = \frac{B_{2c} - B_n}{n} \quad (1)$$

Where, k_f is the stiffness decay rate of the steel fiber concrete beam in the second stage; B_{2c} is the flexural stiffness of the beam at the beginning of the second stage under fatigue loading; B_n is the flexural stiffness of the beam after n cycles. Based on test and calculation results (in Table 6), the stiffness decay rate decreases as the volume rate of steel fibers increases. Compared to high-strength concrete beams without steel fiber, the stiffness decay rate decreased by 42%, 53%, and 60% for 0.5%, 1.0%, and 1.5% of the high strength concrete beams with steel fiber volume fractions respectively. By adding steel fibers to high-strength concrete beams, the rate of stiffness decay can be efficiently controlled, the total damage to the beams during fatigue loading may be minimized, and the beams' lifespan can be extended.

Conclusion

- (1) The primary cause of fatigue damage to steel fiber reinforced high-strength concrete beams, characterized by typical brittle damage characteristics, is fatigue fracture damage to reinforcement in beam members. These characteristics are consistent with those exhibited by ordinary concrete beams. However, the fatigue life of high-strength concrete beams with steel fibers was significantly improved, and the fatigue life of concrete beams containing 0.5%, 1.0%, and 1.5% steel fibers was improved by 66.9%, 132.9%, and 149.9%, respectively, when compared with concrete beams without steel fibers.
- (2) The incorporation of steel fibers demonstrates remarkable effectiveness in enhancing the crack resistance of high-strength concrete beams. Experimental observations reveal that steel fiber-reinforced specimens maintain exceptional toughening characteristics and crack-arresting capabilities even after sustained fatigue loading. This performance enhancement is quantitatively evidenced by two ways: the development of refined and densely distributed microcracks as opposed to the localized macro-cracking observed in plain concrete counterparts, and statistically significant reductions in maximum crack width ranging from 35 to 121% across different loading scenarios when compared to non-fiber control specimens.
- (3) Steel fiber reinforcement demonstrates significant effectiveness in controlling deflection development and mitigating stiffness degradation in high-strength concrete beams subjected to fatigue loading. Comparative analysis reveals that steel fiber-reinforced beams exhibit 15.0–61.0% lower mid-span deflection compared to conventional high-strength concrete counterparts. Furthermore, the stiffness degradation rates in steel fiber-enhanced beams show substantial reductions of 42%, 53%, and 60%, indicating a progressive improvement in structural durability under cyclic loading conditions.

This study, limited by the periodicity of fatigue tests and the complexity of sample preparation, mainly focuses on the influence law of steel fiber volume fraction (0.5–1.5%) on the fatigue performance of high-strength concrete beams. Limited by the sample size the description of the damage evolution at the theoretical model needs to be improved. It is suggested that subsequent studies should be expanded along the following directions: (1) multifactorial coupling effects, including but not limited to the synergistic mechanism of fiber type, concrete strength grade and longitudinal reinforcement ratio; (2) fatigue damage evolution mechanism focusing on the analysis of the crack extension paths and stiffness degradation correlation; (3) residual load carrying performance assessment method and establishment of life prediction model based on energy dissipation coefficient.

Data availability

The data that support the findings of this study are available from the corresponding author upon reasonable request.

Received: 18 November 2024; Accepted: 26 March 2025

Published online: 07 April 2025

References

- Ornum, J. L. V. The fatigue of cement products. *Trans. Am. Soc. Civ. Eng.* **51**, 443–445 (1903).
- Siemes, A. & Van Leeuwen, J. J. I. N. Fatigue of concrete. *Ing. Neth.* **89** (1978).
- Romualdi, J. P. & Mandel, J. A. Tensile strength of concrete affected by uniformly distributed and closed short lengths of wire reinforcement. *ACI J. Proc.* **61** (6), 657–670 (1962).
- Swamy, R. N. & Mangat, P. S. Theory for the flexural strength of steel fiber reinforced concrete. *Cem. Concrete Res.* **4** (2), 313–325 (1974).
- Swamy, R. N. Fiber reinforcement of cement and concrete. *Matériaux Constr.* **8**, 235–254 (1975).
- Ashour, S. A. & Wafa Faisal. Flexural behavior of high strength fiber reinforced concrete beams. *ACI Struct. J.* **90** (3), 279–228 (1993).
- Zhang, P., Wang, C., Gao, Z. & Wang, F. A review on fracture properties of steel fiber reinforced concrete. *J. Build. Eng.* **67**, 105975 (2023).
- Liew, K. M. & Akbar, A. The recent progress of recycled steel fiber reinforced concrete. *Constr. Build. Mater.* **232**, 117232 (2020).
- Trabucchi, I., Tiberti, G., Conforti, A., Medeghini, F. & Plizzari, G. A. Experimental study on steel fiber reinforced concrete and reinforced concrete elements under concentrated loads. *Constr. Build. Mater.* **307**, 124834 (2021).
- Thomas, J. & Ramaswamy, A. Mechanical properties of steel Fiber-Reinforced concrete. *J. Mater. Civ. Eng.* **19** (5), 385–392 (2007).
- Van Chanh, N. Steel fiber reinforced concrete. *Fac. Civil Eng. Ho Chi Minh City Univ. Technol. Semin. Mater.* 108–116 (2004).
- Gao, J. M. & Sun, W. Research on fatigue properties of steel fiber concrete. *Concrete Cem. Prod.* **01**, 10–12 (1989).
- Nanni, A. Fatigue behavior of steel fiber reinforced concrete. *Cem. Concr. Compos.* **13** (4), 239–245 (1991).
- Singh, S. P., Gambhir, M. L. & Kukreja, C. B. Fatigue behavior of fiber reinforced concrete. *Madras India* 603–613 (1991).
- Singh, S. P. & Kaushik, S. K. Fatigue strength of steel fiber reinforced concrete in flexure. *Cem. Concr. Compos.* **25** (7), 779–786 (2003).
- Singh, S. P., Singh, B. & Kaushik, S. K. Probability of fatigue failure of steel fibrous concrete. *Mag. Concrete Res.* **57** (2), 65–72 (2005).
- Deng, Z. Research on compressive fatigue characteristics of steel fiber concrete. *Build. Struct.* **30** (09), 53–55 (2000).
- Deng, Z. Flexural fatigue characteristics of high-performance cellulose fiber and its hybrid fiber concrete. *Highway* **01**, 165–169 (2008).
- Lee, M. K. Barr an overview of the fatigue behaviors of plain and fiber reinforced concrete. *Cement Concr. Compos.* **26**, 299–305 (2004).
- 20 Carlos Zanuy, Pablo & de la Fuente Luis Albajar Effect of fatigue degradation of the compression zone of concrete in reinforced concrete sections. *Eng. Struct.* **29** 2908–2920 (2009).
- Naaman, A. E. & Hammoud, H. Fatigue characteristics of high-performance fiber-reinforced concrete. *Cement Concrete Compos.* **20**, 353–363 (1998).
- Chang, D. & Chai, W. Flexural fracture and fatigue behavior of steel-fiber-reinforced concrete structures. *Nucl. Eng. Des.* **156** (1–2), 201–207 (1995).
- Gao, D., Gu, Z., Wei, C., Wu, C. & Pang, Y. Effects of fiber clustering on fatigue behavior of steel fiber reinforced concrete beams. *Constr. Build. Mater.* **301**, 124070 (2021).
- Gao, D., Gu, Z., Zhu, H. & Huang, Y. Fatigue behavior assessment for steel fiber reinforced concrete beams through experiment and fatigue prediction model. *Structures* **27**, 1105–1117 (2020).
- Li, L., Zeng, Y., Huang, L., Yin, C. & Xu, L. Role of steel fiber on the fatigue behaviors of ultra-high performance concrete containing coarse aggregate. *Constr. Build. Mater.* **460**, 139790 (2025).
- Luo, S., Su, Y., Zhang, Q. & Zhang, K. Effects of steel fibers on the flexural fatigue performance of recycled aggregate concrete. *Construct. Build. Mater.* **412** 134709. (2024).
- Professional Standard of the People's Republic of China. *GB 50152–2012 Standard for Test Methods of Concrete Structures* (China Architecture and Building Press, 2012).
- Feng, X. F. Study on fatigue behavior of P.P.C beams with mixed reinforcement. *PhD Dissertation Dalian Univ. Technol.* (2006).
- Holmen, J. O. Fatigue of concrete by constant and variable amplitude loading. *Fat. Strength Concrete Struct. ACI Publ.* **SP-75**, 71–110 (1982).

Author contributions

All authors contributed to the planning, implementation of the work, and writing the manuscript.

Funding

The work is supported in part by the Science & Technology Program of Anyang (No. 2023C01SF007), in part by the Henan Province Science and Technology Research Project (No. 242102320370), in part by the Key Scientific Research Project of Higher Education Institutions in Henan Province (No. 24B560002) and in part by the 2024 Anyang Normal College Student Innovation and Entrepreneurship Training Program Project (No. 202410479152).

Declarations

Competing interests

The authors declare no competing interests.

Additional information

Correspondence and requests for materials should be addressed to M.Z.

Reprints and permissions information is available at www.nature.com/reprints.

Publisher's note Springer Nature remains neutral with regard to jurisdictional claims in published maps and institutional affiliations.

Open Access This article is licensed under a Creative Commons Attribution-NonCommercial-NoDerivatives 4.0 International License, which permits any non-commercial use, sharing, distribution and reproduction in any medium or format, as long as you give appropriate credit to the original author(s) and the source, provide a link to the Creative Commons licence, and indicate if you modified the licensed material. You do not have permission under this licence to share adapted material derived from this article or parts of it. The images or other third party material in this article are included in the article's Creative Commons licence, unless indicated otherwise in a credit line to the material. If material is not included in the article's Creative Commons licence and your intended use is not permitted by statutory regulation or exceeds the permitted use, you will need to obtain permission directly from the copyright holder. To view a copy of this licence, visit <http://creativecommons.org/licenses/by-nc-nd/4.0/>.

© The Author(s) 2025